Model-Membrane Morphological Transformations Induced by Different Amyloid Molecular Assemblies.

Masamune Morita, Mun'delanji Vestergaard, Tsutomu Hamada and Masahiro Takagi
School of Materials Science, Japan Advanced Institute of Science and Technology,
1-1 Asahidai, Nomi City, Ishikawa 923-1292, Japan

Abstract:

Amyloid beta (Aβ) has been strongly implicated in inducing neurotoxicity in the pathology of Alzheimer's disease (AD). However, the underlying mechanisms remain unknown. In this study, we examined, in real-time, the spatio-temporal changes in individual model membranes induced by the presence of different Aβ-40 molecular assemblies (species). We used cell-sized lipid vesicles to enable the direct observation of these changes. We found two significantly different membrane-transformation pathways. We characterized the biophysical mechanisms behind these transformations in terms of the change in inner vesicle volume and surface area. Interestingly, mature fibrils, which are often considered inert species, also induced profound membrane changes. The real-time observation of these morphological transformations, which can be missed in a discretised analysis, may help to unlock the mechanisms of Alzheimer's Aβ-induced neuro-degeneration.

1. INTRODUCTION

Amyloid beta (Aβ) has been implicated in the pathology of Alzheimer's disease (AD) [1]. Aβ-peptides are a natively unfolded protein that aggregate into a β-sheet structure of ordered fibrils [2]. This fibril formation proceeds from the assembly of monomers into amorphous aggregates, via proto-fibrils, to produce mature fibrils [3]. Some studies have suggested that these intermediates in fibril formation are the most toxic species [4]. Others have suggested that fibrils are the principle triggers of neuronal cell toxicity or disorder [2,5]. Aβ-induced neuronal cell toxicity has been reported to be due to (i) pore formation, (ii) the disruption of ionic channels that could affect calcium homeostasis [2,6], and (iii) lipid peroxidation via membrane-associated free radical formation [7]. Thus, the actual mechanism of Aβ-induced neuronal cell toxicity remains unclear.

There has been extensive research on the role of Aβ in AD. Some research groups have studied the interactions between Aβ and lipids [8]. Lipid and cholesterol compositions have been reported to affect oligomerisation and reverse ('backward') oligomerisation [9]. Small and large lipid vesicles (< μm) have also been used to study the influence of a lipid bilayer on Aβ-peptide assembly [10]. Most studies on the interaction between Aβ-peptides and lipid vesicles have concentrated on how the composition of the membranes affects peptides, and particularly how levels of cholesterol and different lipid compositions in a given model membrane affect oligomerisation and assembly of the peptides [11]. Based on the results of these studies, there have been many suggestions regarding how different Aβ molecular species cause neurotoxicity, mainly based on the use of histochemical dyes [9] rather than on the direct real-time observation of the biological or model membranes being studied.

Our focus is different from these previous studies in that we are directly studying membrane responses to the presence of Aβ-peptides. Specifically, we used cell-sized (>10 μm) model membranes to directly observe the spatio-temporal changes in individual vesicles. These biomimetic membranes enable the researcher to manipulate a 'biological' micro-vesicle under a controlled environment [12,13]. In this study, we examined the interaction of different oligomeric species of Aβ-40 with a lipid vesicle, while observing changes in membrane morphology, in real time using a simple phase-contrast microscope.

2. MATERIALS AND METHODS

2.1 Materials

Amyloid β-40 HiLyte Fluor™ 488-labeled, Anaspec, Amyloid β-40 (trifluoroacetate salt) was purchased from Peptide Institute Inc., (Osaka, Japan), 1,2-Dioleoyl-sn-Glycero-3-Phosphocholine (DOPC) was obtained from Avanti Polar Lipids, mica disks were from Furuuchi Chemical Co. (Tokyo, Japan),. All other chemicals were purchased from Wako Pure Chem. Co. (Japan).

2.2 Preparation of Giant Unilamelar Vesicles (GUV) and Observation Using an Optical Microscope.

DOPC lipid was dissolved in chloroform / methanol (1:1 v/v) mixture. DOPC solution was transferred into a glass tube and gently dried using stream of nitrogen gas, to produce a thin lipid film. The thin film was subsequently dried under vacuum overnight, and was hydrated with ultrapure Milli Q (18 Ω) for 3 hours at 37 ℃. The final lipid concentration was 0.5 mM. Four μL of this vesicle solution was placed on a glass slide and examined using a phase-contrast microscope (Olympus BX-51, Japan).

978-1-4244-5095-4/09/$26.00 ©2009 IEEE

2.3 Imaging Amyloid β-40 assembly using Atomic force microscopy (AFM).

Aβ-40 was taken out from incubation, and samples were diluted with Milli Q to a final concentration of 8 µM. Immediately after, the peptide was immobilised on clean mica disk (Furuuchi Chemical Co., Shinagawa, Tokyo, Japan). AFM images were obtained using an AFM unit (SPA400-SPI3800, Seiko Instruments Inc., Chiba, Japan) equipped with a calibrated 20 µm xy-scan and 10 µm z-scan range PZT-scanner and a silicon nitride tip (SI-DF40P, spring constant = 42 N/m, frequency resonance = 300 kHz, Seiko Instruments Inc.) was used for AFM imaging of samples. All AFM images were obtained in air in a dynamic force mode (DFM mode) at optimal force. All AFM operations were done in an automated moisture control box with 30-40% humidity at RT.

2.4 Association and Localisation of Aβ-40 on GUVs.

HiLyte Fluor™ 488-labelled Aβ-40 and Aβ-40 was mixed 1:2 (mol ratio). Aβ-40 was added to lipid vesicles to a final concentration of 2 µM. Four µL of this solution was imaged using a confocal microscope (Olympus FV-1000, Japan).

2.5 Interaction of Aβ-40 with GUVs.

Amyloid β was incubated at 37 ^{o}C in 20 mM Tris buffer, pH 7.4 at 80 µM concentration for various incubation periods. After incubation, Aβ was was introduced to lipid vesicles at a final concentration of 2 µM in 0.5mM Tris buffer, by dilution in Milli Q water. Immediately after addition, the vial containing the lipid vesicles and Aβ were mixed gently by tapping. Observation of the vesicular dynamics was within 2 min of peptide introduction to the lipid vesicles. Real-time observation of Aβ-40-vesicle interaction was observed as above, for total period of 20 min.

2.6 Treatment with osmotic stress.

Lipid vesicles and 2 mM glucose solution were poured into a test tube and gently mixed by tapping. Observation of the vesicular dynamics was within 2 min of glucose solution introduction to the lipid vesicles.

3. Results and Discussions

First, we incubated 80 µM Aβ-40 in 20 mM Tris, pH 7.4 (Tris) at 37 ^{o}C for various periods. Immediately after incubation, Aβ-40 (2 µM) was added to cell-sized lipid vesicles composed of dioleoyl-phosphatidylcholine (DOPC), and their interaction was observed in real-time. As shown in Figure 1A, pre-fibrillar Aβ localised on the membrane surface, and interacted with the vesicle.

Fluctuation of the membrane was the first response to the presence of the Aβ-peptide. As shown in Figure 1B, after addition of the peptide, the dynamic movements of the vesicles were observed and calculated the degree of membrane fluctuation.

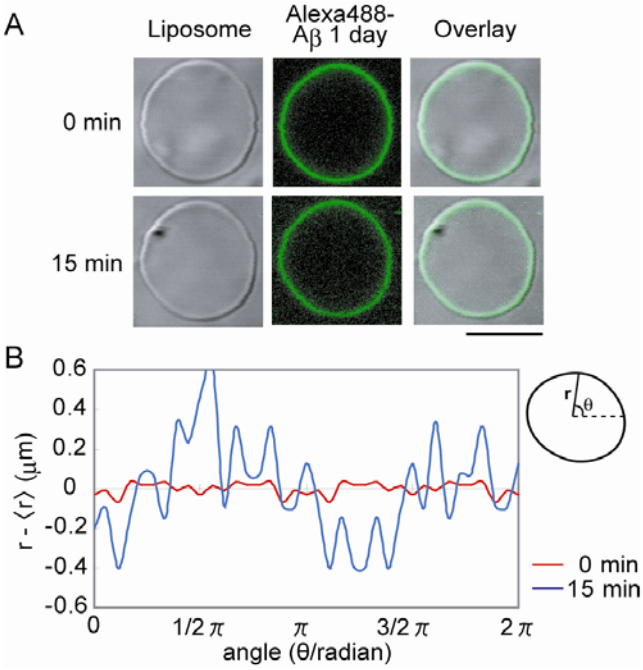

Figure 1A. Differential interference image of vesicles (left) and only fluorescence Aβ-40 image (center) and overlay image (right).B Fluctuation degree of 0 min and 15 min vesicles.

We captured two distinct lipid vesicular transformation pathways induced by different Aβ-40 species. Interestingly, mature fibrils, which have often been considered to be inert species, also induced profound changes in membrane morphology. In addition, pre-fibrillar species induced a transformation that led to an increase in the membrane surface area. First, we incubated Aβ-40 in 20 mM Tris, pH 7.4 (Tris) at 37 ^{o}C for various periods. Immediately after incubation, Aβ-40 (2 µM) was added to cell-sized lipid vesicles composed of dioleoyl-phosphatidylcholine (DOPC), and their interaction was observed in real-time. Some vesicles did not show any changes in the presence of the peptide, while others exhibited fluctuations that culminated in shape changes (Fig.2). Some vesicles formed large sphero-stomatocyte (Fig.2A), while others formed small sphero-stomatocyte (Fig. 2B), at the end of the vesicular transition. In fact, the lipid vesicles exhibited two distinct pathways to these changes in membrane morphology. A slower ('slow membrane dynamics') and included more

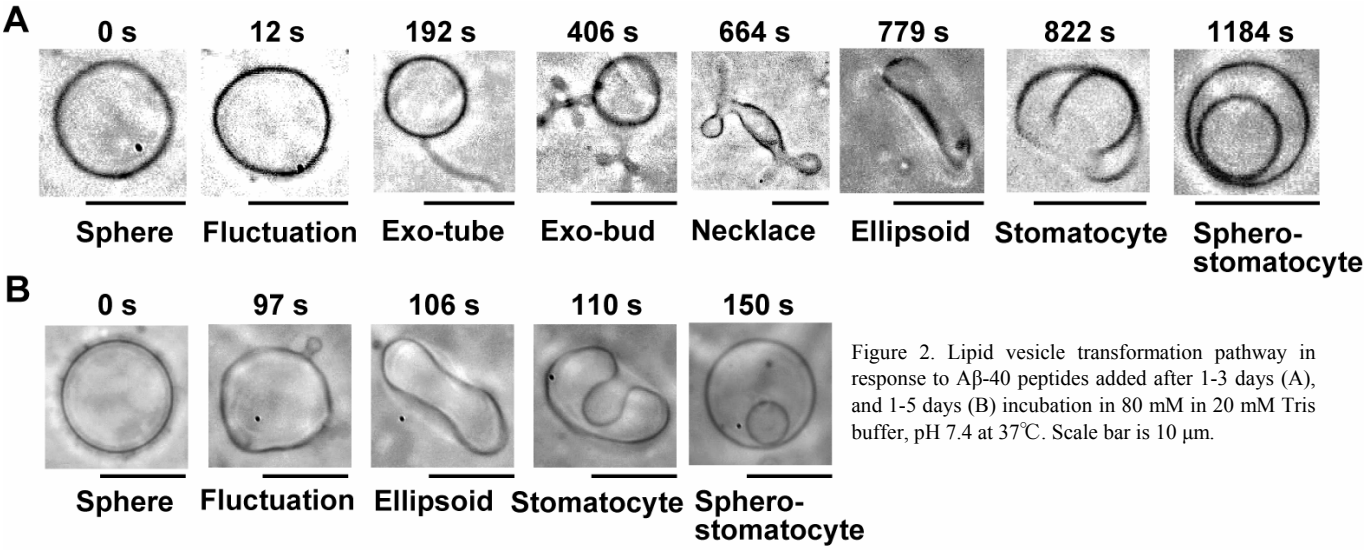

Figure 2. Lipid vesicle transformation pathway in response to Aβ-40 peptides added after 1-3 days (A), and 1-5 days (B) incubation in 80 mM in 20 mM Tris buffer, pH 7.4 at 37℃. Scale bar is 10 μm.

stages before reaching the 'final' sphero-stomatocyte stage (Fig. 2A). The sphero-stomatocyte was larger than that formed under the slow membrane dynamics. The sphero-stomatocyte was formed after 21.4 min (n=5; SD=6.4). The second pathway was transformed into an ellipsoid, then into a stomatocyte, and finally into a small sphero-stomatocyte within a relatively short time (mean 3.24 min; n=8; SD=1.69). We called this pathway 'fast membrane dynamics' (Fig. 2B).

The effect of osmotic stress and how it induces membrane fluctuation and morphological changes has been reported [14]. To gain a better understanding of the observed Aβ-induced morphological changes, we investigated the behavior of our membrane system under osmotic stress. We observed membrane morphological transformations. The osmotic stress pathway was fast (3.5 min), and culminated in a vesicle with a very small sphero-stomatocyte. This was very similar to the fast membrane dynamics (Fig. 2(B)).

The relationship between morphological changes in the membrane and the degree of Aβ assembly is also of interest (Fig. 3A). Typical AFM images of Aβ-40 solutions show the state of different oligomeric species at specific time-points in incubation (Fig. 3B). The images show small to large oligomeric species after 0 and 1 day, respectively. Proto-fibrillar species start to appear after 2 days, and then elongate to form mature fibrils observed after 4 to 5 days of incubation. The slow dynamics was observed only after the addition of Aβ-40 that had been incubated for 1, 2 and 3 days, i.e., pre-fibrillar species. The fast dynamics was observed for all Aβ-40 species, except for that which was introduced to vesicles immediately after peptide preparation.

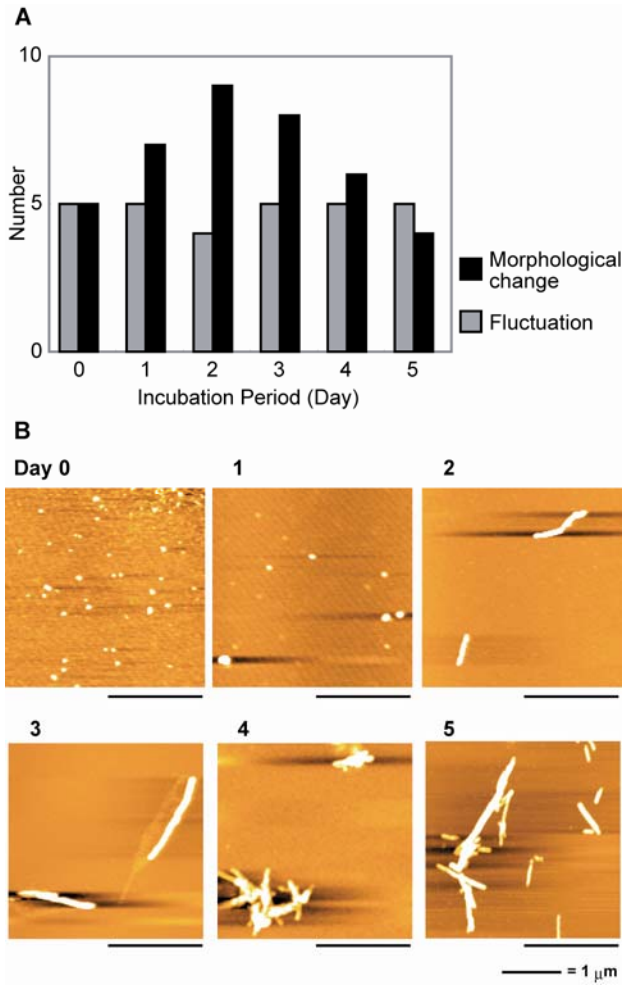

Figure 3A Response of DOPC lipid vesicle to the addition of Aβ-40 peptides that were incubated for the indicated time periods. B Atomic force microscopy images of Aβ-40 after incubation at 80 mM in 20 mM Tris buffer, pH 7.4, at 37℃ for 0 (0), 1 (1), 2 (2), 3 (3), 4 (4), and 5 days (5).

We characterized the vesicular transformations in terms of the increase in excess surface area. The excess area is a parameter that describes the membrane morphology in terms of Helfrich bending energy, and is defined by a dimensionless variable ξ as a function of the membrane surface area A and vesicular volume V [14, 15]. We calculated the surface area and volume changes just after addition of the peptide and just after sphero-stomatocyte formation. Figure 4 shows the dimensionless excess area ξ of the obtained sphero-stomatocyte vesicles and the radius of the sphero-stomatocyte r divided by R_0 (initial vesicular radius).

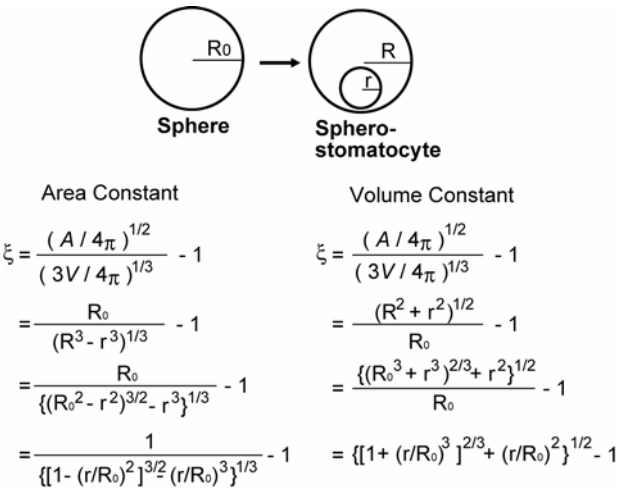

Figure 4. Dimensionless excess area ξ of the transformed vesicles obtained sphero-stomatocyte vesicles and the radius of the sphero-stomatocyte r divided by R_0 (initial vesicular radius).

The two membrane dynamics induced by Aβ-40 are clearly different. The slow dynamics showed a statistically significant increase in ξ compared to the fast dynamics, as a result of (i) a decrease in the inner vesicle volume (28%), and (ii) an increase in surface area (35%, n=5). The fast dynamics showed no change in area (0.2%; n=8), while there was a 13% decrease in mean volume. This decrease in the inner volume could be caused by an efflux of aqueous material, as is typical under osmotic stress. The increase in surface area by the pre-fibrillar-induced change in morphology is itself intriguing.

Fibrils are attracted to, albeit with low affinity, and interact briefly with lipids. The interaction of rigid fibrils with a soft DOPC membrane may change the spontaneous curvature of the membrane to initiate membrane fluctuation. An increased fluctuation intensity may cause the vesicular transformation as the membrane attempts to re-gain a favourable low-energy state. Engel et al. [16] showed a similar change in membrane shape, which later changed back to the original shape. In addition, we captured changes in the vesicle interior. The formation of an sphero-stomatocyte could influence the spatial localization of membrane proteins such as receptors. The slow dynamics caused an increase in surface area. Pre-fibrillar Aβ, which have high affinity for lipids, interacted with them, and were eventually inserted into the bilayer. The packing of lipid molecules became sub-optimal, and this resulted in the creation of small gaps [17]. Furthermore, we propose that Aβ-40 interacted with free lipids and/or small vesicles outside the giant vesicles and incorporated them into the mother vesicle. The uptake of lipids by amyloids from vesicles has been previously reported [18]. Since DOPC is a zwitterionic lipid, the interactions between Aβ-40 and DOPC membrane were hydrophobic-driven. The polar OH group of a tyrosine residue and its hydrophobic ring structure are suitable for localization at the water:lipid interface, which would provide an anchor for the peptide.

4. Conclusions

Our results provide clear evidence that Aβ-peptides cause membrane damage by drastically changing the membrane morphology. This is the first clear demonstration of real-time spatial-temporal changes in membrane dynamics induced by different Aβ species.

Acknowledgements

We thank Dr. M. Hatakeya (Jaist) for valuable discussion.

References

[1] Walsh, D. M., and D. J. Selkoe. 2004. Deciphering the molecular basis of memory failure in Alzheimer's disease. *Neuron.* 44:181-193.

[2] Stefani, M., and C. M. Dobson. 2003. Proteinaggregation and aggregate toxicity: new insights into protein folding misfolding diseases and biological evolution. *J. Mol.Med.* 81(11):678-699.

[3] Pellarin, R., E. Guarnera, and A. Caflisch. 2007.Pathways and intermediates of amyloid fibril formation. *J. Mol. Biol.* 374:917–924.

[4] Bucciantini, M., Giannoni, E., Chiti, F., Baroni, F.,Formigli, L., et al. 2002. Inherent toxicity of aggregatesimplies a common mechanism for protein misfolding diseases. *Nature.* 416: 507-511.

[5] Lorenzo, A., and B. A. Yankner. 1996. Amyloid fibril toxicity in Alzheimer's disease and diabetes. *Ann. N Y. Acad. Sc.* 777:89-95.

[6] Arispe, N., E. Rojas, and H. B. Pollard. 1993.Alzheimer disease amyloid beta protein forms calcium channels in bilayer membranes: blockade by tromethamine and aluminum. *Proc. Natl. Acad. Sci. USA.* 90:567-571.

[7] Butterfield, D. A., J. Drake, C. Pocernich, and A. Castegna. 2001. Evidence of oxidative damage in Alzheimer's disease brain: central role for amyloid β-peptide. *Trends Mol. Med.* 7:548-554.

[8] Chauhan, A., I. Ray, and V. P. S. Chauhan. 2000 Interaction of amyloid beta-protein with anionic phospholipids: possible involvement of lys28 and c-terminus aliphatic amino acids. *Neurochem. Res.* 25:423-429.

[9] Martins, I. C., I. Kuperstein, H. Wilknson, E. Maes, M. Vanbrabant, et al. 2008. Lipids revert inert Aβ amyloid fibrils to neurotoxic protofibrils that affect learning in mice. *Eur. Mol. Biol. J.* 27:224-233.

[10] Kakio, A., S. Nishimoto, K. Yanagisawa, Y.Kozutsumi,and K. Matsuzaki. 2001. Cholesterol-dependent formation of GM1 ganglioside-bound amyloid β-protein, an endogenous seed for Alzheimer amyloid. *J. Biol. Chem.* 276:24985-24990.

[11] Rojo, L., M. K. Sjoberg, P. Hernandez, C. Zambrano and R.B. Maccioni. 2006. Roles of cholesterol and lipids in the etiopathogenesis of Alzheimer's disease. *J. Biomed. Biotech.* 1-17

[12] Vestergaard, M., T. Hamada, and M. Takagi. 2008. Using model membranes for the study of amyloid beta:lipid interactions and neurotoxicity. *Biotech. Bioeng. J.* 99:753-763.

[13] P. L. Luisi, and P. Walde. 2000. Giant Vesicles. John Wiley and Sons Ltd, England.

[14] Ishii, K., T. Hamada, M. Hatakeyama, R. Sugimoto, T. Nagasaki, et al. 2009. Reversible control of exo- and endo-budding transitions in a photo-sensitive membrane. *ChemBioChem*. 10:251-256.

[15] Dobereiner H.G. 2000. Properties of giant vesicles. *Curr. Opin. Coll. Interface Sci.* 5:251-256.

[16] Engel, M. F., L. Khemtemourian, C. C. Kleijer, H. J. Meedijk, J. Jacobs, et al. 2008. Membrane damage by human islet amyloid polypeptide through fibril growth at the membrane. *Proc. Natl. Acad. Sci. USA.* 105(16):6033-6038.

[17] Friedman, R., R. Pellarin and A. Caflisch. 2009. Amyloid aggregation on lipid bilayers and its impact on membrane permeability. *J. Mol. Biol.* In press.

[18] Sparr, E., M. Engel, D. Sakharov, M. Sprong, J. Jacobs,et al. 2004. Islet amyloid polypeptide-induced membrane leakage involves uptake of lipids by forming amyloid fibers. *FEBS Lett.* 577:117-120.